

NEUTRON SCATTERING INVESTIGATION ON TREHALOSE, MALTOSE AND SUCROSE/H₂O MIXTURES

S. Magazù, G. Maisano, F. Migliardo

Dipartimento di Fisica and INFN, Università di Messina, PO Box 55, I-98166 Messina, Italy

(Received December 10, 2004; received in final form April 11, 2005)

New Inelastic Neutron Scattering (INS) results obtained by using the TOSCA spectrometer (ISIS Facility, Rutherford Appleton Laboratory, UK) on disaccharides/H₂O mixtures are presented. The comparison among the spectra of trehalose, maltose and sucrose/H₂O mixtures, besides evidencing a different destructuring effectiveness on the H₂O hydrogen bond network, and hence different *cryoprotectant* properties, shows a higher “crystallinity” degree for the trehalose/H₂O system which accounts for its higher “rigidity”. This result justifies the better *cryptobiotic* action of trehalose in respect to maltose and sucrose.

Key words: inelastic neutron scattering, vibrational properties, disaccharides, bioprotection.

PACS number(s): 61.12.Ex, 61.25.Hq, 63.50.+x

I. INTRODUCTION

In recent years many efforts have addressed the understanding of the tools used by organisms to survive under environmental stress conditions [1–3]. Prominent examples of these survival mechanisms are found in some species of frogs that are able to survive to relatively low temperatures for weeks by means of natural cryoprotective agents that include low-molecular-weight substances such as polyhydric alcohols (commonly glycerol) and sugars (e. g., trehalose), and high-molecular-weight proteins that inhibit ice formation [2–5]. Tardigrades are another class of organisms able, thanks to the synthesis of trehalose, to live in extreme conditions, such as temperatures near absolute zero and above the boiling point of water, very high pressures, a hard vacuum, high doses of radiation [6–7]. In particular, they are able thanks to trehalose to reversibly suspend their metabolism and to enter in a particular state called “cryptobiosis” (from Greek *κρυπτος*, “hidden”, “concealed” and *βιος*, “life”). The environmental extreme conditions determine which of four cryptobiotic pathways (anhydrobiosis, cryobiosis, osmobiobiosis, and anoxybiosis) will occur [6–7]. For this reason trehalose has been revealed itself both a very effective *cryoprotective* and *cryptoprotectant* agent.

A wide presence of trehalose in nature as a bioprotector has suggested its playing a role of as stabilizer of cellular structures. In accordance with this suggestion, several studies have shown an outstanding property of trehalose in protecting proteins [8], biological membranes and enzymes under conditions of dehydration and elevated temperatures [9].

The bioprotective effects of trehalose have suggested manifold promising applications, such as those in preserving vaccines and mammalian cells during drying or cryopreservation, and biological macromolecules like DNA during radiation exposure [10–11].

In this frame it is well known that water plays a key role in living systems thanks to its unique properties and

also to its “anomalies”. One of these is its particular behaviour when it cools. When liquid water is cooled, it contracts until the temperature of approximately 4°C is reached; after that, it expands slightly until it reaches the freezing point, and then when it freezes it expands by approximately 9%. The physiological damages induced by ice on the living organisms are due to this expanded structural arrangement that destroys cells and tissues.

Although the trehalose *cryoprotectant* and *cryptoprotectant* effectiveness is proved, the underlying molecular mechanisms are not fully clarified so far. Crowe and coworkers [12] have formulated a hypothesis that direct interaction between the sugars and the object of protection occurs. More specifically, their “water replacement hypothesis” asserts the existence of a hydrogen bonding of trehalose with polar headgroups of the lipids that constitute biomembranes, which could explain the trehalose protective function. However, different spectroscopic techniques [13–23] and the density function theory simulation [24] indicate that a preferred trehalose-water interaction takes place.

In more detail, previous inelastic light scattering [13–14] findings by means of the well-known decomposition of Raman spectra into an “open” contribution, attributed to the O–H vibration in tetrahedrally bonded H₂O molecules that have an “intact bond”, and a “closed” contribution, corresponding to the O–H vibration of H₂O molecules that have a not fully developed hydrogen bond (“distorted” bond) have shown that the addition of trehalose rapidly destroys the intermolecular network of water.

Neutron diffraction data [23] show a strong distortion of the significant peaks in the partial radial distribution functions $g_{HH}(r)$ and in $g_{XX}(r)$ with a shift which can be attributed to the destructuring of the tetrahedral coordination of pure water.

Moreover, ultrasonic velocity measurements [14] have evidenced that, in respect to the other disaccharides, the trehalose–water system is characterized, in all the investigated concentration range, by both the highest value of the interaction strength and of the hydration number.

Finally, the density functional theory [24] has provided for the disaccharide–H₂O systems a detailed picture for the interpretation of the Infrared and neutron vibrational spectral features.

The aim of this work is to investigate by INS the vibrational behaviour of trehalose, maltose and sucrose/H₂O mixtures in order to characterize the structural changes induced by disaccharides on the H₂O hydrogen-bonded network. The obtained neutron scattering findings yield evidence to the effect that disaccharides in general have a destructuring effect on the pure H₂O hydrogen bonded network, and that trehalose, in particular, among the investigated sugars, results the best “structure breaker”. Moreover, neutron scattering spectral profiles show that by lowering the H₂O content trehalose/H₂O mixtures show in respect to maltose/H₂O and sucrose/H₂O mixtures a higher crystalline behaviour.

II. EXPERIMENTAL SECTION

Trehalose, maltose and sucrose show a different structural arrangement: trehalose and maltose are composed by two glucose rings linked by an oxygen glycosidic bond whose orientation is different for the two sugars, whereas sucrose is formed by a glucose ring and a furanose ring linked by a similar oxygen glycosidic bond.

Vibrational spectra of disaccharides/H₂O mixtures at $T = 27$ K have been collected by the indirect geometry time-of-flight (t.o.f.) spectrometer TOSCA at the ISIS Pulse Neutron Facility (DRAL, UK) [25] in the energy range $0 \div 4000$ cm⁻¹ ($0 \div 500$ meV) with the best results below 2000 cm⁻¹ (250 meV). For the scattering geometry of TOSCA, the effective scattering angle 2θ for all pencils of radiation backscattered from the sample is 135° , so that $\cos 2q = \mathbf{k}_f \times \mathbf{k}_0 / k_f \times k_0 = -1/\sqrt{2}$ and $Q^2 = k_f^2 [2 + v + (1 + v)^{1/2} \sqrt{2}]$; $v = \eta\omega/E_f$, where $E_f = 31.86$ cm⁻¹ is the “final” or (fixed) analyser energy. During the inelastic neutron scattering experiment, the scattered neutrons are energy-analysed by means of Bragg-scattering from a large array of single crystals (pyrolytic graphite or mica). Only those neutrons with the appropriate wavelength/energy to satisfy the Bragg condition are directed towards the detector bank. A consequence of the indirect geometry is that for energy transfers > 100 cm⁻¹ the momentum transfer vector is essentially parallel to the incident beam. The significance is that for an INS transition to be observable there must be a component of motion parallel to the momentum transfer vector. This means that with oriented samples measurements directly analogous to optical polarisation experiments can be carried out [25–26].

By this spectrometer both the collective excitations region at low frequency and the localized excitations region at the intermediate and higher frequency region can be covered [25–26]. TOSCA’s resolution (in the whole energy range of interest, the instrument provides very good energy resolution, about $\Delta E/E \approx 1.5 \div 2\%$, which is comparable with optical techniques such as IR and Raman spectroscopies), combined with a high intensi-

ty of the ISIS source, allows to perform a study of the dynamic with high accuracy, reducing the background noise/signal ratio down to negligible for strongly scattering samples [25–26].

Trehalose, maltose and sucrose water mixtures at different concentration values were prepared starting from ultrapure samples purchased from Aldrich-Chemie and doubly-distilled deionized water. For all the investigated hydrogenated samples, the measurement time was 12 hours for each run. For the sample preparation, thin walled aluminium cells have been used. The samples were cooled to 27 K by a liquid helium cryostat. Care was taken to obtain stable, clear and dust-free samples; ample time was allowed for equilibration.

For the data treatment a small amount of flat background from the empty-cell measured at similar conditions was subtracted from the measured data. The measured INS data were transferred to the dynamical structure factor $S(Q, \omega)$ vs energy transfer by using a standard data treatment program. For what concerns the Debye–Waller factor that strongly influences the spectral intensity, its effect is reduced by collecting the INS spectra at low temperature. The multiple scattering contribution has been minimised by using a thin sample in order to obtain a scattering transmission from the sample $> 90\%$. The usual one-phonon expression for high ω and low T values reduces to [27]:

$$S(Q, \omega) = \frac{Q^2 \cdot B_\omega}{3} \cdot \exp(-Q^2 \cdot \alpha_\omega) \quad (1)$$

where $\alpha_\omega = \frac{1}{5} \left\{ \frac{TrA}{3} + 2 \frac{B_\omega \cdot A}{TrB_\omega} \right\}$ and $A = \sum_\omega B_\omega$. The observed intensity $S(Q, \omega)$ of a band at the frequency ω is a function of the momentum transferred Q (determined by spectrometer) and the vibrational amplitude B_ω of the hydrogen atoms that can be extracted.

Since the incoherent neutron scattering cross-section for hydrogen atom is much larger than the other atoms, for hydrogen containing materials, due to annihilation of l and creation of $(k - l)$ excitations, we obtain [27–29]:

$$\begin{aligned} S(Q, E) &= \sum_{l,k} S_{l,k-l}(Q, E) \\ &= \sum_{l,k} \frac{\sigma_{\text{H}}^{\text{inc}}}{4\pi} \exp[-2W(Q)] \\ &\quad \times \left(\frac{\hbar^2 Q^2}{2m_n} \right)^k \int d\omega_1 \dots d\omega_k \frac{G(\omega_1) \dots G(\omega_k)}{\omega_1 \dots \omega_k (k-l)!!} \\ &\quad \times \prod_{i=l+1}^k [n(\omega_i) + 1] \prod_{j=1}^l n(\omega_j) \\ &\quad \times \delta \left(E - \sum_{i=l+1,k} \hbar\omega_i + \sum_{j=1,l} \hbar\omega_j \right) \end{aligned} \quad (2)$$

with $n(\omega)$ population Bose factor, m_n neutron mass, $W(Q)$ Debye–Waller factor for hydrogen atom,

$$W(Q) = \frac{1}{2} \langle (Qu)^2 \rangle = \frac{\hbar^2}{12m} \int \frac{Q^2 G(\omega)}{\omega} [2n(\omega) + 1] d\omega$$

and $G(\omega)$ generalized vibrational density of states for hydrogen atom.

The multiphonon neutron scattering contribution (MPNS) has been evaluated by means of an iterative technique based on the assumption that the one-phonon term describes the INS spectrum at the lower energy transfers and on the calculation of the first MPNS term for the whole energy region from this first step. The result is a new one-phonon spectrum that will allow to get with successive iterative calculations MPNS terms until good convergence is obtained [27–29].

III. RESULTS AND DISCUSSION

INS spectra of ice can be subdivided into two different regions: i) the region of the H_2O intermolecular vibrations up to $\sim 960 \text{ cm}^{-1}$, in which one distinguishes a “translational” part up to $\sim 400 \text{ cm}^{-1}$ and a “librational” part, ii) the region of the H_2O intramolecular vibrations up to $\sim 3600 \text{ cm}^{-1}$, that presents the bending modes at $\sim 1600 \text{ cm}^{-1}$ and the stretching modes at $\sim 3360 \text{ cm}^{-1}$ [27–29].

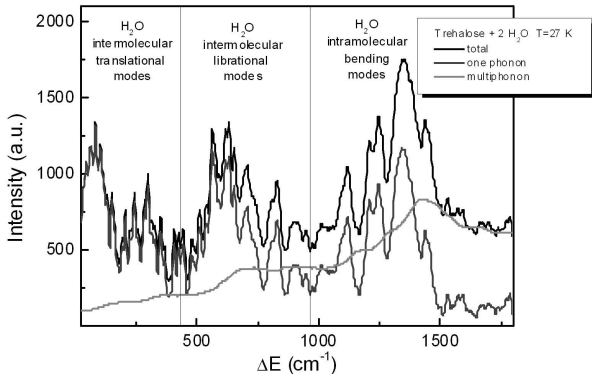


Fig. 1. INS spectrum of trehalose/ H_2O mixture at a concentration value corresponding to 2 H_2O molecule for each disaccharide molecule with the multiphononic correction. The black line is the total spectrum, the blue line is the one phonon contribution, the red line is the multiphonon contribution.

As far as the INS spectra of disaccharides/ H_2O mixtures are concerned, Figure 1 shows, within the spectral frame of ice, the spectrum of trehalose/ H_2O mixture at a concentration value corresponding to 2 H_2O molecules

for each disaccharide molecule together with the MPNS correction. As can be seen, this correction does not affect significantly the translational modes region at low frequency, but increases at larger energy transfer.

More specifically, taking into account the different spectral regions, the following features can be observed:

i) $0 \div 200 \text{ cm}^{-1}$ region

This spectral region concerns with low energy collective modes. No significant difference is observed for the three disaccharides/ H_2O mixtures: as an example, the peak at $\sim 54 \text{ cm}^{-1}$ in the ice spectrum, associated with the distortion of the local structure due to the topological disorder, is equivalently depressed by the three disaccharides.

ii) $200 \div 1060 \text{ cm}^{-1}$ region

As already mentioned, in this region for ice two different contributions to the intermolecular modes can be distinguished: translational and librational modes, respectively. The spectra of the disaccharides/ H_2O mixtures in the region $200 \div 400 \text{ cm}^{-1}$, see for example Figure 2, where spectra relative to a concentration of 19 H_2O molecules for each disaccharide molecule reported, are all dominated by ice.

Important differences for the three disaccharides are observed in the $400 \div 1060 \text{ cm}^{-1}$ region. It was found that the characteristic value for the librational band in the INS spectrum for different ice forms is the position of its low-energy cut-off [27–29]. Assuming the moment of inertia for water molecules in the ices is about the same, the observed shifts of the cut-off position indicate that the transverse forces between the water molecules are of different intensity for the different ice forms. In Figure 3 an extension of the cut-off region for disaccharide/ H_2O mixtures is reported.

We observe that in the ice spectrum the position of this cut-off is at $\sim 544 \text{ cm}^{-1}$, whereas for the investigated mixtures we find for its position the value of $\sim 547 \text{ cm}^{-1}$ for trehalose and maltose and of $\sim 544 \text{ cm}^{-1}$ for sucrose. This circumstance clearly indicates that trehalose and maltose influence more than sucrose the interactions among different H_2O molecules. On the other hand, the intensity increase at the cut-off for ice is ~ 3.61 , whereas for trehalose, maltose and sucrose ~ 1.84 , ~ 1.91 and 2.03 , respectively.

Furthermore the C–O stretching found in the trehalose spectrum by simulation [24] at $\sim 1000 \text{ cm}^{-1}$ does not appear, indicating that this kind of modes in the rings is hindered because of the presence of hydrogen bonds with water.

These findings suggest that all the disaccharides modify significantly the spectral features of ice in this spectral region. In particular trehalose shows a smaller value of its intensity increase and a larger shift of its position, this circumstance indicating that it affects more than the other disaccharides the intermolecular interaction forces, and the arrangements of the H_2O molecules, as already evidenced by Raman and IR spectroscopy [13,14]. On the other hand, sucrose has no effect on the position, but it changes in intensity, evidencing, however, a small effect.

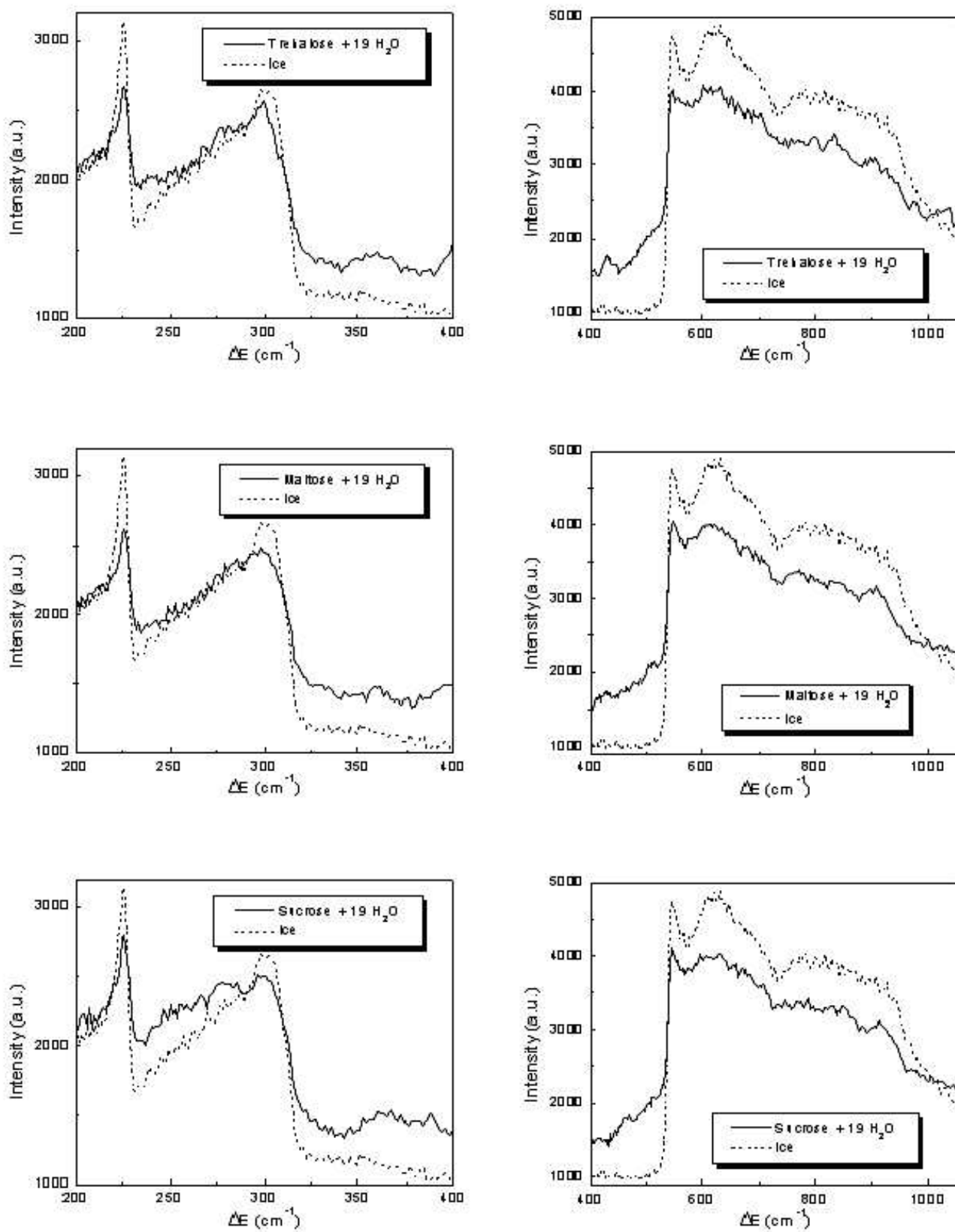


Fig. 2. INS region 200÷1060 cm⁻¹ of disaccharides/H₂O mixtures.

Since the attention is focused on the disaccharide–H₂O interaction, all these results justify a greater effectiveness of trehalose as structure-breaker of the hydrogen bonded network of ice.

iii) 1060÷2000 cm⁻¹ region

The intensity profile of trehalose/H₂O mixture in this spectral region which corresponds to the range of the bending vibrational modes of ice appears more “structured” in comparison with the other disaccharides and in particular with sucrose, this latter showing a more smooth trend.

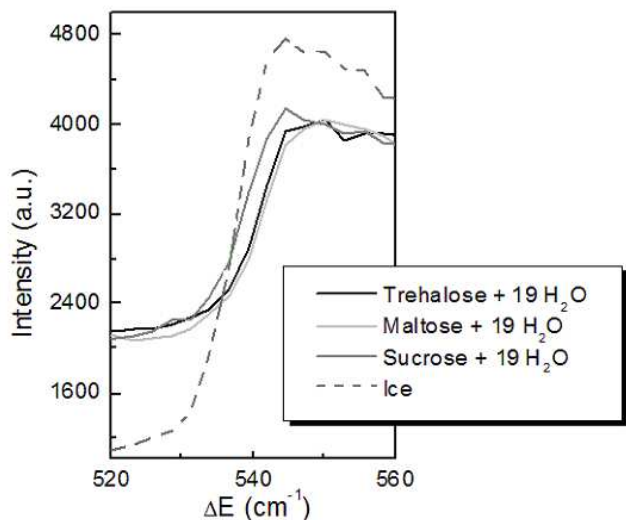


Fig. 3. Comparison of INS spectra of EG and PEGs in the region of the D-LAM contributions.

In Figure 4 a comparison among trehalose, maltose and sucrose/H₂O mixtures in the spectral bending region is reported. We maintain these comparisons are necessary for evidencing the strong interaction of the H₂O molecules with disaccharides, in particular with trehalose.

Since from these results it is not possible to extract quantitative information about the changes induced by trehalose on the H₂O structural arrangement, we can take into account the DFT simulation results in order to assign the observed peaks to significant modes of the investigated system. Following the simulation results [24] the stretching of the C–O bonds occurs in the range between 960 and 1104 cm⁻¹, whereas the band of the hybridized H–C–H, C–C–H and C–O–H bending modes is present between 1160 and 1440 cm⁻¹. A striking feature characterizing the simulation results consists in the evaluation of the conformational freedom in the trehalose molecule: the results show that a relatively low energy is required for the torsions around the oxygen linking the two rings to occur, whereas the bending of the same angle is much less likely, being energetically unfavourable. When the interaction with water is introduced through the simulation of the trehalose crystal with two trehalose monohydrate molecules in the unit cell, apart from some expected distortions in the O–H bonds of wa-

ter molecules, the most apparent difference between the vibrational spectra of the crystal and of the molecules concerns the modes localized on the OH groups. The C–H stretching band is relatively unchanged in frequency, but it has broader implications. At 1600 cm⁻¹ the bending of water appears. Below this energy the differences between a single molecule and the crystal are quantitatively small [24].

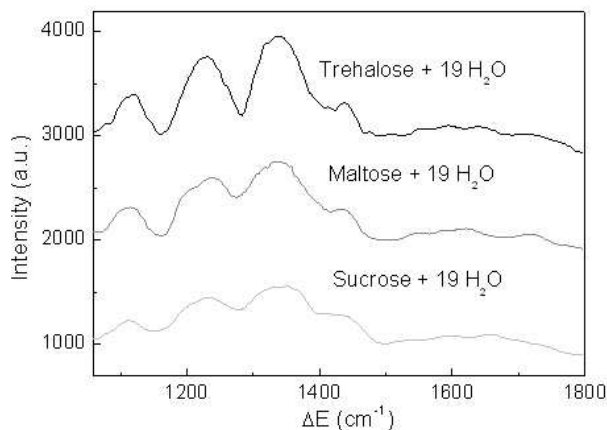


Fig. 4. INS region 1060÷2000 cm⁻¹ of disaccharides/H₂O mixtures.

By an inspection of Figure 4 it is evident that trehalose shows more distinctly, in respect to the other disaccharides, the characteristic peaks typical of the crystalline state described above. In other terms the trehalose/H₂O complex shows a more “crystalline” behaviour, namely a locally more ordered structure, which can justify a higher rigidity of this system [18]. Trehalose, besides modifying significantly the structural and dynamical properties of water, forms with H₂O a more rigid unique entity able to encapsulate biological structures and to protect them in a more rigid environment. In our opinion this circumstance is relevant because it implies a better *cryptobiotic* effect and hence a higher capability of bioprotection at high disaccharide concentration.

IV. CONCLUSIONS

In this paper new INS results on disaccharides/H₂O mixtures are shown. The whole body of data evidences the effects of disaccharides on the vibrational properties of ice. In more detail we observe that:

1. Whereas the translational modes of H₂O molecules are not significantly influenced by the presence of disaccharides, the librational modes are increasingly modified by sucrose, maltose and trehalose, as particularly evidenced by the position shift and intensity increase of the low-energy cut-off. This finding can justify a higher *cryoprotectant* effectiveness of trehalose.

2. Trehalose affects more significantly the structural arrangements of the neighbouring H₂O molecules by means of a more “crystalline” conformation. This circumstance could explain the trehalose *cryp-*

toprotectant effectiveness: by interacting with water, trehalose is able to create more rigid structures able to adapt the trehalose/H₂O complex to the irregular surface of the biostructures.

-
- [1] A. Hirsh, *Cryobiology* **24**, 214 (1987).
 [2] K. B. Storey, J. M. Storey, *Annu. Rev. Physiol.* **54**, 619 (1992).
 [3] R. E. Jr. Lee, J. P. Costanzo, E. C. Davidson, J. R. Jr. Layne, *J. Therm. Biol.* **17**, 263 (1992).
 [4] L. K. Miller, *Comp. Biochem. Physiol.* **59 A**, 327 (1978).
 [5] R. Zentella, J. O. Mascorro-Gallardo, P. Van Dijck, J. Folch-Mallol, B. V. Bonini, C. Vaeck, R. Gaxiola, A. A. Covarrubias, J. Nieto-Sotelo, J. M. Thevelein, G. Iturriaga, *Plant Physiol.* **119**, 1473 (1999).
 [6] J. H. Crowe, A. F. Jr. Cooper, *Sci. Am.* **225**, 30 (1999).
 [7] W. R. Miller, *Tardigrades: Bears of the Moss*, Kansas School Naturalist 43:3, 1 (1997).
 [8] K. Gekko, S. N. Timasheff, *Biochemistry* **20**, 4667 (1981).
 [9] G. M. Fahy, *Prog. Clin. Biol. Res.* **224**, 305 (1986).
 [10] K. Yoshinaga, H. Yoshioka, H. Kurosaki, M. Hirasawa, M. Uritani, K. Hasegawa, *Biosci., Biotech. Biochem.* **61**, 160 (1997).
 [11] N. Saita, N. Fujiwara, I. Yano, K. Soejima, K. Kobayashi, *Infect. Immun.* **68**, 5991 (2000).
 [12] J. H. Crowe, L. M. Crowe, D. Chapman, *Science* **223**, 701 (1984).
 [13] C. Branca, S. Magazù, G. Maisano, P. Migliardo, *J. Chem. Phys.* **111**, 281 (1999).
 [14] C. Branca, A. Faraone, S. Magazù, G. Maisano, F. Migliardo, P. Migliardo, V. Villari, *Rec. Res. Develop. in Phys. Chem.* **3**, 361 (1999).
 [15] C. Branca, S. Magazù, F. Migliardo, P. Migliardo, *Physica A* **304**, 314 (2002).
 [16] C. Branca, S. Magazù, G. Maisano, F. Migliardo, G. Romeo, *Appl. Phys. A* **74**, 450 (2002).
 [17] C. Branca, S. Magazù, G. Maisano, F. Migliardo, G. Romeo, *J. Phys. Chem. B* **105**, 10140 (2001).
 [18] C. Branca, A. Faraone, S. Magazù, H. D. Middendorf, F. Migliardo, P. Migliardo, *Physica B* **301**, 126 (2001).
 [19] C. Branca, S. Magazù, G. Maisano, F. Migliardo, *Phys. Rev. B* **64**, 224204 (2001).
 [20] C. Branca, S. Magazù, G. Maisano, F. Migliardo, G. Romeo, *Philos. Mag. B* **82**, 347 (2002).
 [21] C. Branca, S. Magazù, G. Maisano, F. Migliardo, G. Romeo, *J. Phys. Chem.* **105**, 2612 (2001).
 [22] C. Branca, A. Faraone, S. Magazù, F. Migliardo, P. Migliardo, V. Villari, *J. de Physique IV* **10**, 329 (2000).
 [23] C. Branca, S. Magazù, G. Maisano, F. Migliardo, *Rec. Res. Develop. in Phys. Chem.* **6**, 35 (2002).
 [24] P. Ballone, N. Marchi, C. Branca, S. Magazù, *J. Phys. Chem.* **104**, 6313 (2000).
 [25] D. Colognesi, S. F. Parker, *The TOSCA Manual*, Rutherford Appleton Laboratory UK (1999).
 [26] D. K. Breiting, J. Mohr, D. Colognesi, S. F. Parker, H. Schukow, R. G. Schwab, *J. Mol. Struct.* **563**, 377 (2001).
 [27] A. I. Kolesnikov, J. C. Li, N. C. Ahmad, C.-K. Loong, M. Nipko, L. Yocum, S. F. Parker, *Physica B* **263**, 650 (1999).
 [28] A. I. Kolesnikov, J. C. Li, S. F. Parker, R. S. Eccleston, C.-K. Loong, *Phys. Rev. B* **59**, 3569 (1999).
 [29] J. C. Li, *J. Chem. Phys.* **105**, 6733 (1996).

ВИВЧЕННЯ НЕЙТРОННОГО РОЗСІЮВАННЯ НА СУМІШАХ ТРЕГАЛОЗИ, МАЛЬТОЗИ, ЦУКРОЗИ/H₂O

С. Магацц, Г. Маїзано, Ф. Мільярдо

Університет Мессіни, фізичний факультет, РО Вох 55, Мессіна, I-98166, Італія

Подано нові результати щодо нееластичного нейтронного розсіювання, які отримано завдяки застосуванню спектрометра TOSCA (Rutherford Appleton Laboratory, Великобританія), дисахаридів/H₂O та сумішей цукрози/H₂O. Порівняння спектрів трегалози, мальтози та сумішей цукрози/H₂O, окрім різної деструктуризаційної ефективності щодо мережі водневих зв'язків H₂O, виявляє вищий ступінь кристалічності для системи трегалози/H₂O. Цей факт пояснює вищу “жорсткість” такої системи. Наш результат дає підстави вести мову про ліпшу криптобіотичну дію трегалози порівняно з мальтозою та цукрозою.